Crown Ether-Functionalized Complex Emulsions as an Artificial Adaptive Material Platform

Saveh Djalali, Pablo Simón Marqués, Bradley D. Frank, and Lukas Zeininger*

Responsive materials capable of autonomously regulating and adapting to molecular recognition-induced chemical events hold great promise in the design of artificial chemo-intelligent life-like soft material platforms. In this context, the design of a synthetically minimal artificial emulsion platform that, regulated by interfacial supramolecular recognition events, is capable to autonomously and reversibly adapt to its chemical environment is reported. The systems exhibit programmed up- and down-regulating capabilities that are realized via selective assembly of synthesized crown ether surfactants onto one hemisphere of anisotropic biphasic emulsion droplets. Dynamic and reversible interfacial host–guest complexation of, for example, metal and ammonium ions or amino acids transduce into interface-triggered morphological reconfigurations of the complex emulsion droplets, which mediate their ability to selectively present, hide, or expand liquid–liquid interfaces. The separate responsive modalities are then used to showcase the utility of such adaptive soft material platforms for a self-regulated uptake and release of metal ions or phase-transfer catalysts, a biomimetic recognition of biomolecules including amino acids, carbohydrates, and antibodies, and for triggered surface-encoded payload release applications.

1. Introduction

Autonomous regulation of supramolecular recognition and binding-induced chemical events are essential processes through which natural systems exert control over complex biological functions. Beyond being responsive, that is, exhibiting a programmed response to a specific chemical or physical signal, living organisms can dynamically adapt their response to multiple parallel and independent triggering events and changes in their chemical environment.[1] As a result, chemical information can be processed with high fidelity and highest substrate specificities are achieved as multiple individual or combinations of independent chemical equilibrium-driven non-covalent interactions and covalent chemical transformations are translated into a specific response.[2] This cross-check capability and self-regulation behavior forms the basis for the high complexity and specificity achieved within biological systems and is further fundamental for complex emergent behavior observed in multibody systems, for instance their self-regulated ability to communicate, move, evolve, and self-organize into patterns or networks.[3] An emulation of the individual capabilities within synthetically minimal, biomimetic model systems may help to better understand the underlying complex cascade mechanisms and pave the way toward artificial dynamic and self-regulatory adaptive systems.[4]

The constant fluid transport and mass exchange between cells that is autonomously controlled and driven through a continuous exchange of ions across the lipophilic cellular membranes is an example of such a self-regulation of multiple independent chemical events. The ion exchange is essential for maintaining the hydrostatic and osmotic pressure balance as well as the membrane potential.[5] Moreover, beyond these basic functions, the recognition and transport of specific ions is also an important biomarker to many physiological and pathological processes, including the perception of taste, or for signaling, for example, in nerves and muscle cells.[6] As opposed to an active transport that requires an external physical stimuli,[7] passive ion exchange is solely driven by chemical concentration gradients and chemical binding equilibria whereby the transport through the lipophilic membrane barrier can be enabled by membrane proteins or ionophores.[8] The latter have been successfully mimicked using artificial ionophores, such as synthetic crown ether-based compounds.[9] Similarly to natural ionophores, crown ethers can complexate metal ions within their hydrophilic binding pocket to enable a phase-transfer and transport of hydrophilic ions through a lipophilic phase.[10] Thus, crown ethers provide an exciting avenue to impart materials with responsive behavior, a concept that has been elegantly designed and used in a variety of applications, including in supramolecular polymers, micelles, protection groups, phase-transfer catalysis, or molecular motors.[11]

The continuous exchange of chemical information within biological systems and thus their associated multifunctional, chemo-intelligent behavior emerges from their complex and functional

S. Djalali, P. Simón Marqués, B. D. Frank, L. Zeininger
Department of Colloid Chemistry
Max Planck Institute of Colloids and Interfaces
Am Muehlenberg 1, 14476 Potsdam, Germany
E-mail: lukas.zeininger@mpikg.mpg.de

**ADVANCED
SCIENCE NEWS**
www.advancedsciencenews.com

**ADVANCED
FUNCTIONAL
MATERIALS**
www.afm-journal.de

out-of-equilibrium assembled nature.[12] Therefore, a bio-inspired generation of an active and adaptive, ideally autonomously operating self-regulated material platform requires combining the concept of responsivity with a functional and stable out-of-equilibrium material platform. In this context, complex emulsions, kinetically stabilized phase-separated dispersions of fluids, offer a versatile platform as they persist in a thermodynamically out-of-equilibrium state and are highly dynamic.[13] In surfactant stabilized emulsion droplets, molecules are continually exchanged between droplets and the continuous phase and these metastable colloids can be influenced by a variety of chemical and physical triggers.[14] The multiphase emulsions used in this study, comprise of two fluids that are phase separated at room-temperature, and thus exhibit multiple exquisitely sensitive interfaces. The micro-scale bi-phasic emulsion droplets can be dynamically reconfigured as their internal morphology is solely controlled by the force-balance of interfacial tensions acting at the individual interfaces.[15] Thus far, such variations in the droplet shape are typically evoked by externally triggering changes in the surfactant effectiveness rendering them a broadly programmable stimuli-responsive material platform for refractive, reflective, and light-emitting optical components,[16] droplet-based imaging systems,[17] as structural templates for the generation of precision objects,[18] or as transducers in chemo- and biosensing platforms.[19] While many of these applications rely on the ability to controllably configure and optimize specific droplet morphologies, droplets that can autonomously adapt their configuration to their chemical environment, independently controlled by two or more chemical equilibrium-driven molecular recognition events, provide a new avenue in the creation of adaptive organized complex liquid colloids en route toward the generation of life-like cell-sized soft materials that display autonomous chemo-intelligent capabilities.

In this study, we explore a novel concept for the generation of soft materials that can adapt their response to multiple independent chemical triggering events. Specifically, we demonstrate the generation and manipulation of biphasic oil-in-water emulsions that are anisotropically functionalized with crown ether moieties. Through combination of multiple reversible and competitive interfacial host–guest complexation events with the intrinsic reconfigurability of dynamic double emulsions we yield a synthetically minimal material system that can be actuated and adapt its internal droplet morphology to different independent chemical-equilibrium controlled pathways, including the presence of metal ions, ammonium compounds, or amino acids as well as variations in the surfactant composition or effectiveness (**Scheme 1**). We showcase the implications of such an adaptive complex emulsion system, for example, in controlling the reactivity inside droplet microreactors, for bioconjugation, and controlled surface-encoded payload release applications.

2. Results and Discussion

The bi-phasic emulsion droplets used in this study were comprised of a hydrocarbon (toluene; hereafter: HC) and a fluorocarbon oil (mixture of HFE-7500 and FC-43; hereafter: FC). The distinct oil mixture was selected because it phase-separates at room temperature, however exhibits a convenient upper critical solution temperature of $T = 32\ °C$ and thus could be employed for the generation of complex double emulsions using an established thermal phase-separation approach.[20] Generated droplets were characterized by a very low internal interfacial tension ($<0.5\ mNm^{-1}$) between the two oil phases as compared to significantly higher interfacial tensions between the oils and the aqueous surfactant-containing continuous phase ($> 5.0\ mNm^{-1}$). As a result, droplets assume a spherical shape with an internal droplet morphology that can be fine-tuned via balancing interfacial tensions at the external droplet interfaces.
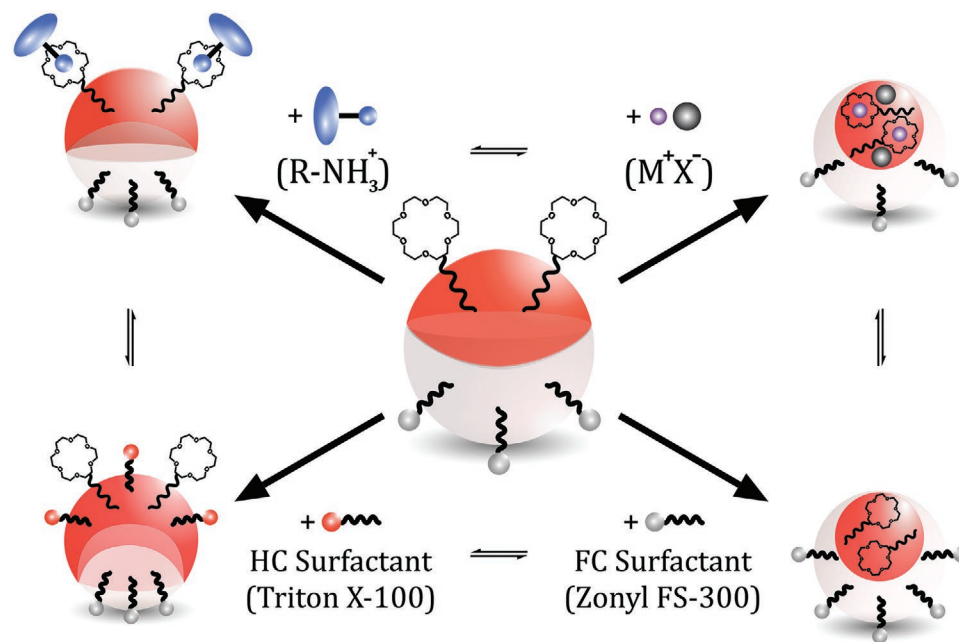
Scheme 1. Schematic side-view illustration of independent competitive chemical equilibrium-controlled molecular recognition events causing morphological reconfigurations of crown ether-functionalized complex double emulsions.

2107688 (2 of 9)
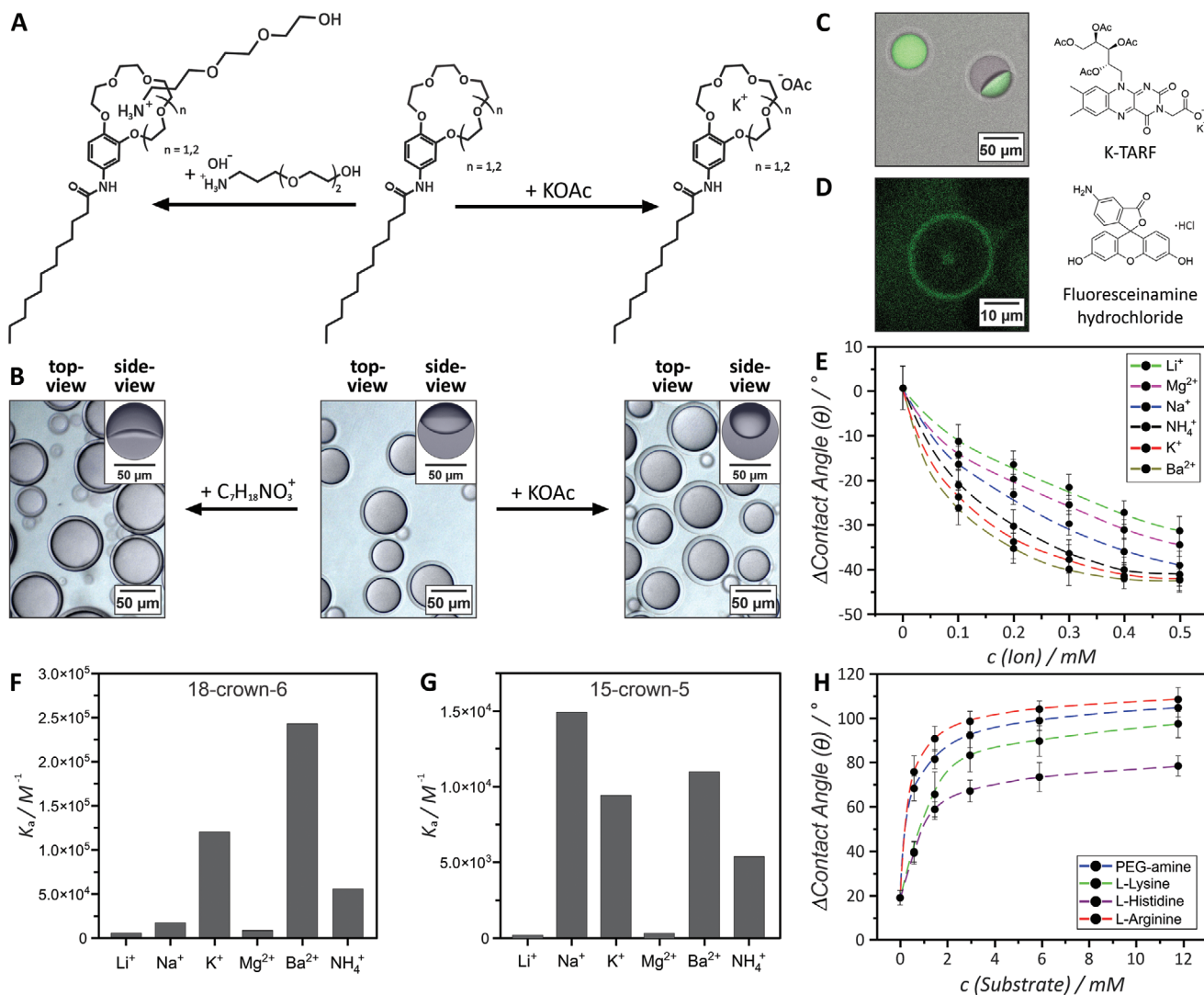
Figure 1. A) Chemical structure of the 4'[*N*-dodecanoylamino]benzo-15-crown-5 and 4'-[*N*-dodecanoylamino]benzo-18-crown-6 surfactants and their ability to complexate metal ions and ammonium compounds. B) Side- and top view micrographs of the morphological transitions evoked by the different molecular recognition events: Complexation of a hydrophilic ammonium compound (left) and encapsulation of potassium acetate (right). C) Confocal micrograph of droplets after phase-transfer of the fluorescent marker K-TARF. The image shows strong emission in the hydrocarbon phase. D) Confocal micrograph of a droplet after the complexation of fluoresceinamine hydrochloride. The image shows a bright fluorescent ring selectively located at the HC/W interface. E) Droplet morphological transition upon addition of metal and ammonium ions. Encapsulation of several metal and ammonium salts performed with the 18-crown-6 surfactant. Calculated association constants for the interfacial complexation of different metal and ammonium ions by the F) 18-crown-6 and the G) 15-crown-5 surfactants. H) Droplet morphological transition upon complexation of different hydrophilic amino acids and ammonium compounds. Contact angle standard deviations are based on $N \geq 10$ measurements.

Employed HC- and FC-surfactants, namely, Triton X-100 and Zonyl FS-300, ensure droplet stability and variations in their ratio allowed to controllably modulate the internal droplet geometry between encapsulated and Janus morphologies.

In addition to the commercial surfactants, we employed two different synthesized crown ether-based surfactants, 4'[*N*-dodecanoylamino]benzo-15-crown-5 and 4'-[*N*-dodecanoylamino] benzo-18-crown-6 (**Figure 1**A).[21] The molecules possessed an intrinsic amphiphilicity due to the hydrophilic crown ether head groups, which were attached to hydrophobic alkyl tails. Both, the 15-crown-5 and 18-crown-6 surfactants, formed micelles above a concentration of 3.73 and 5.32 mM, respectively, and effectively lowered the water-toluene interfacial tension comparable

to other commercial nonionic surfactants ($\approx$14.6 mNm^{-1} and $\approx$11.8 mNm^{-1} above the respective critical micelle concentration; Figures S13 and S14, Supporting Information).

Two-phase emulsion droplets prepared with the crown ether surfactants assumed an 'opened up' Janus morphology even when prepared within a pure Zonyl (0.05 wt%)-containing aqueous continuous phase, that is, without an addition of subsidiary hydrocarbon surfactants. This could be attributed to a selective assembly of the crown ether surfactants at the hydrocarbon-water interface of the droplets. To quantitatively describe the resulting droplet morphologies we determined the contact angle at the triple phase contact line (Figure S1, Supporting Information) using a customized side-view imaging

setup. Horizontal micrographs of the droplets prepared with the 15-crown-5 surfactants (4 mg mL^{-1}) resulted in a contact angle of the droplets of $\theta = 21.2 \pm 2.7°$ whereas we observed an increase in the contact angle to $\theta = 40.72 \pm 4.9°$ for droplets generated using the 18-crown-6 surfactants (4 mg mL^{-1}), attributed to the larger hydrophilic head group and therefore an increased surfactant effectiveness of the latter. Figure 1B displays top- and side-view micrographs of crown ether-functionalized double emulsions in their natural gravity-aligned orientation with the denser FC-phase at the bottom.

In Janus emulsions, variations in the balance of interfacial tensions transduce into morphological reconfigurations. When employing the as-prepared crown ether-functionalized droplets, we observed that different interfacial supramolecular host–guest recognition events could lead to two opposite morphological transitions. Upon addition of an inorganic metal salt, such as potassium acetate, droplets transitioned from their Janus configuration into an encapsulated double emulsion morphology ($\theta = 0°$). Crown ether moieties are known to form hydrophobic complexes upon coordination to suitable metal ions, which resulted in a phase transfer of the metal salts into the organic phase. Thus, the reduced effectiveness of the crown ether surfactants led to an increase of the hydrocarbon-water interfacial tension. The complexation was reversible, that is, upon decreasing the concentration of metal ions in the continuous phase via dilution, the emulsion droplets reversibly adapted to their environment via expanding the HC/W interface ultimately returning to the starting droplet morphology. In contrast, the addition of the hydrophilic 2-[2-(3-aminopropoxy)ethoxy]ethan-1-ol, was followed by a further 'opening up' of the Janus droplet morphology toward contact angles of $\theta > 90°$, which corresponds to a decrease of the HC-W interfacial tension. In this scenario, complexation of the hydrophilic ammonium compounds led to an increase of the hydrophilic-lipophilic balance of the surfactant, resulting in a more effective surfactant. Horizontal imaging allowed to in situ visualize both droplet morphological transitions evoked by the different molecular recognition events (Figure 1B).

The proposed transitions could be further evidenced by recording confocal micrographs of droplets after complexation of two different fluorescent markers. Complexation of potassium 2-(7,8-dimethyl-2,4-dioxo-10-((2S,3S,4R)-2,3,4,5-tetraacetoxypentyl)-4,10-dihydropyrimido[4,5-b]quinolin-3(2H)-yl)acetate (K-TARF) yielded double emulsion droplets with the dye compartmentalized within the hydrocarbon phase, due to the associated crown ether-mediated phase-transfer of the metal salt (Figure 1C). In turn, an addition of fluoresceinamine hydrochloride, a water-soluble ammonium compound, resulted in confocal micrographs that displayed a bright fluorescent ring located selectively at the HC-W interface of the droplets, due to the interfacial post-functionalization of the crown ether-functionalized emulsions (Figure 1C).

We next set out to quantify the ability of crown ether-functionalized double emulsions to detect different metal and ammonium ions. Therefore, we monitored the droplet response upon addition of different types and concentrations of metal and ammonium salts. Horizontal imaging of the droplets allowed to visually follow in situ the molecular recognition events and quantify association constants via determination of

the associated changes in the droplet contact angle ($\Delta\theta$). Upon interfacial recognition of different metal ions, droplet contact angles gradually decreased with higher salt concentrations. Depending on the cavity size of the two different crown ethers, droplets functionalized with the 15-crown-5 surfactant rapidly transitioned into a fully encapsulated morphology upon addition of small concentrations (0.5 mM) of sodium acetate. The highest affinity of the 18-crown-6 surfactant was determined toward barium acetate, a trend that was in accordance to the binding affinities of the two crown ethers reported in the literature.[22] The association constants for the interfacial complexation of the different metal ions by the two crown ether surfactants were obtained by non-linear regression of the morphology transition graphs (Figure 1E and Figure S18, Supporting Information) using the following equation[23]:

$$\Delta\theta = \frac{1}{2}\left([G]+[H]_0+\frac{1}{K_A} \right) - \sqrt{\left([G]+[H]_0+\frac{1}{K_A} \right)^2 + 4[H]_0 \times [G]} \quad (1)$$

With $K_A = \frac{[HG]}{[H][G]}$: association constant; $[G]$: metal ion concentration; $[H]$: crown ether concentration, $\Delta\theta$: change in droplet contact angle. As a result, the highest association constant of the 18-crown-6 surfactant were determined for barium acetate $K_A = 2.43 \times 10^5$ M^{-1} (Figure 1F). Among different alkali metal ions, the calculated constants document the intrinsic affinities of the 15-crown-5 surfactant toward the smaller sodium ions ($K_A = 1.49 \times 10^4$ M^{-1}). In comparison, the 18-crown-6 surfactant displayed higher affinities toward larger potassium ions ($K_A = 1.20 \times 10^5$ M^{-1}).

Similarly, we also tracked the attachment of different hydrophilic amino acids that are present as zwitterionic compounds at pH = 7 and therefore exhibit a NH$_3^+$ functionality. The 18-crown-6 ether-functionalized emulsions visually responded to the presence of L-lysine, L-hystidine, and L-arginine. Upon complexation, the contact angles and thus the HC-W-interface increased as a function of the hydrophilicity of the respective amino acids (Figure 1H). In analogy to the complexation of metal ions, association constants for the binding of amino acids and the ammonium compound 2-[2-(3-aminopropoxy)ethoxy]ethan-1-ol (PEG-amine) were determined to $K_A = 1088$ M^{-1} for L-lysine, $K_A = 1346$ M^{-1} for L-hystidine, $K_A = 3463$ M^{-1} for L-arginine and $K_A = 2468$ M^{-1} for the PEG-amine.

The two opposite molecular recognition-induced droplet morphological reconfigurations were solely driven by the respective chemical equilibrium constants. Therefore, the respective concentrations determined the degree of competitive binding of both, metal ions and hydrophilic ammonium compounds. Synonymously, when amino acids were added to the crown ether-functionalized droplets disposed within a more concentrated aqueous salt solution (1 mM), droplets retained their encapsulated morphology. Vice versa, upon addition of 0.1 mM potassium acetate to an emulsion functionalized with L-arginine at high concentrations (12 mM), droplets retained their 'opened-up' Janus morphology. Beyond the crown ether-mediated variations in the droplet morphology, all double emulsion droplets retained their ability to respond to variations in the ratio and concentration of other, non-stimuli-responsive HC- and FC-surfactants. As an example, an increase of the Zonyl concentration within the continuous phase from 0.05 to 1.0 wt% resulted
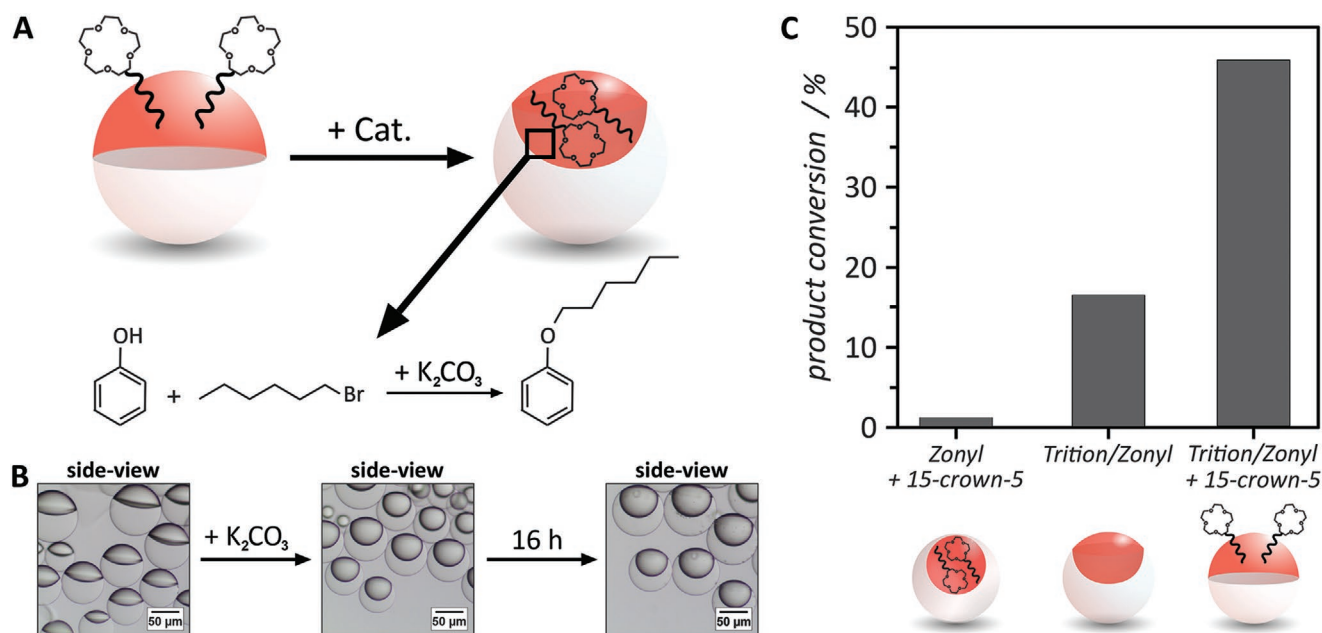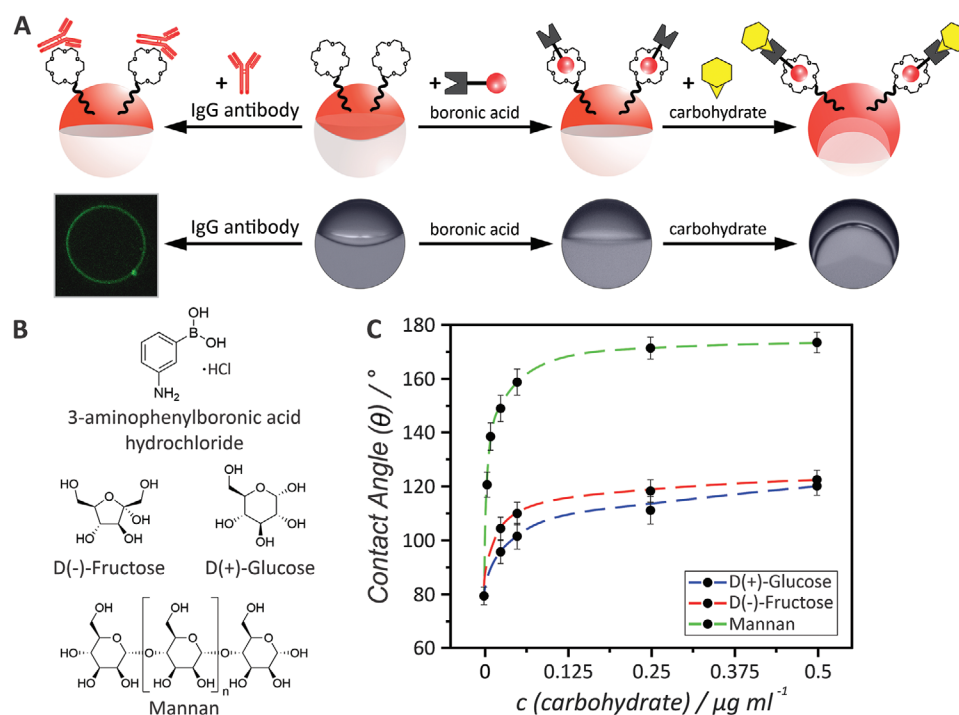
Figure 2. A) Schematic representation of crown-ether functionalized Janus droplets as phase-transfer catalysis microreactors for an alkylation of phenol; B) Optical side-view micrographs of the Janus droplet microreactors, functionalized with the 15-crown-5 surfactant before and after the addition of the catalyst K_2CO_3 as well as after a reaction time of 16 h. C) Product conversion under three different experimental conditions determined after a reaction time of 16 h.

in a decrease of the FC-W-interfacial tension and therefore a transition toward an encapsulated double emulsion morphology with the HC-phase encapsulated by the FC-phase, thus obstructing interfacial supramolecular recognition or post-functionalization events (Figure S20, Supporting Information).

Having validated the responsivity of crown ether-functionalized double emulsion droplets to small molecule triggers, we next set out to explore the implications of the associated chemical equilibrium-driven and adaptive behavior of the emulsion morphology in response to more functional components, thus broadening the supramolecularly regulated uptake and release mechanisms for potential applications. Emulsion droplets are widely employed as droplet-based microreactors,[24] and we therefore hypothesized that the droplet morphology-dependent uptake of a catalytic reagent can be used to control a chemical reaction rate inside the droplets. In this context, we opted for a K_2CO_3-catalyzed alkylation of phenol using 1-bromohexane (**Figure 2**A).[25] First, droplets functionalized with the 15-crown-5 surfactant (6 mM) were prepared in an aqueous surfactant solution (0.02 wt% Triton/0.05 wt% Zonyl) that contained phenol (0.21 M) and 1-bromohexane (0.21 M) selectively compartmentalized inside the HC-phase of the double emulsions. Then, the K_2CO_3 catalyst (0.02 M), that was insoluble in the HC-phase, was added to the continuous phase. The catalyst uptake was accompanied by a morphological reconfiguration toward a more encapsulated morphology, as displayed in Figure 2B. As a result, when crown ether-functionalities were exposed to the catalyst-containing continuous phase, a transfer to the organic phase occurred, resulting in an acceleration of the reaction rate. After 16 h of reaction, the emulsion was de-emulsified with brine, extracted with hexane and analyzed by GC-MS. The received chromatogram revealed a yield of the final product (*p*-(hexyloxy)benzene ether) of 46% when crown ether-functionalities were in contact with the continuous phase (Figure 2C). In turn, a reaction performed inside Janus droplet microreactors under the same reaction conditions without the presence of crown ether surfactants resulted in significantly decreased conversion rates after 16 hours of 18% yield. In analogy to the results described above, we observed that the crown ether-mediated phase-transfer of the catalyst depended on the droplet morphology, which could be independently regulated by variations in the Zonyl concentration within the continuous phase. The same reaction performed inside encapsulated double emulsion droplets prepared in pure Zonyl (1.0 wt%) gave no conversion to the final product, outlining the importance of the reactant-containing HC-phase being exposed to the catalyst-containing aqueous phase (Figures S21–27, Supporting Information).

Next, we were also interested in using the crown ether-functionalized droplets to probe interactions with biomacromolecules. Here, we were motivated to extend the results on the morphology-dependent spontaneous and reversible supramolecular interfacial coupling of amino acids toward a supramolecular interfacial post-conjugation with other functional amines and proteins to develop a potential material platform for the generation of biosensors. Protein- and carbohydrate-modified dynamic double emulsions have recently attracted large interest as powerful transducers for liquid-based biosensing platforms, including for the rapid detection of antibodies, bacterial pathogens, and viruses.[26] In these previous reports, proteins and carbohydrates were conjugated to the oil-water interface using covalent or dynamic covalent bioconjugation schemes, which required a targeted engineering of particular surfactants and droplet platforms toward a specific target. In this context, a
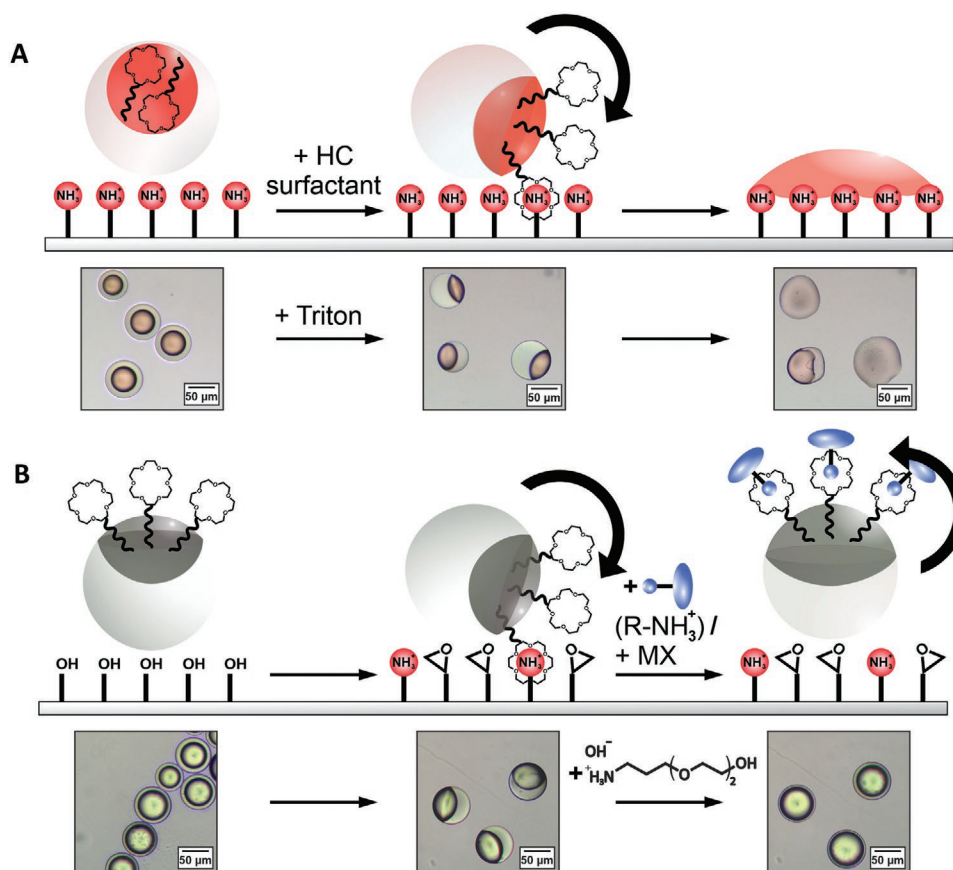
Figure 3. A) Schematic representations and micrographs of the supramolecular bioconjugation schemes. The confocal micrograph displays a bright fluorescent ring, proving the successful conjugation of the FITC-labeled antibodies selectively to the crown ether-functionalized hemisphere of the Janus emulsion. B) Chemical structures of the boronic acid and the carbohydrates used for the carbohydrate complexation schemes. C) Janus droplet morphological reconfiguration in response to varying concentrations of added carbohydrates. Contact angle error bars refer to $N \geq 10$ measurements.

reversible and straightforward supramolecular conjugation of functional cellular recognition units, such as antibodies, to a universal droplet platform may help to expand the capabilities of Janus emulsion biosensor arrays that provide for advanced sensitivities as they more closely resemble the dynamic interfacial recognition processes at the interface of natural cells. In this context, we conjugated the crown ether-functionalized droplets with a fluorescent FITC-conjugated human IgG antibody via simple addition to the aqueous continuous phase (2.67×10^{-4} mM). Bioconjugation with the antibodies led to an expansion of the HC/W interface of the droplet (from 74° to 102°), due to the increased hydrophilicity of the resulting assembly. In addition, the attachment of the antibodies was confirmed using confocal micrographs, which displayed a bright fluorescent ring showing the successful conjugation of the antibodies selectively to one hemisphere of the crown ether-functionalized Janus droplets (**Figure 3**A). In the control experiment, which was carried out under the same conditions but in absence of the 18-crown-6 surfactant, no fluorescence emission at the HC/W interface was detected, confirming the key role of crown ether-functionalities in the bioconjugation mechanism (Figures S28 and S29, Supporting Information).

Next, we endeavored a post-functionalization of the crown ether surface functionalities with boronic acid-based carbohydrate receptors through NH_3^+ mediated complexation by addition of 3-aminophenylboronic acid hydrochloride (0.2 mM). Next to proteins, carbohydrates play an important role in many physiological and pathological processes and synthetic boronic acid-based receptors are well known for this compound class.[27] Boronic acids form reversible 1,2- and 1,3-complexes with diols

and therefore we observed a pronounced reconfiguration of the droplet shape upon addition of the carbohydrates D(+)-Glucose and D(-)-Fructose. Complexation of the polysaccharide Mannan caused the strongest change in droplet morphology as a result of its hydrophilicity and multivalency and resulted in almost fully encapsulated HC/FC/W double emulsions ($\theta = 173°$) (Figure 3).

In addition, the independent chemical equilibrium-controlled interfacial recognition of functional groups and the associated translation into dynamic droplet responses were leveraged to trigger a manipulation or destruction of double emulsions upon interaction with solid interfaces. Based on the unique ability of the droplets to selectively present and hide reactive liquid interfaces we endeavored to demonstrate an interaction with surface-encoded functionalities. Therefore, we initially placed droplets that were submerged in a pure Zonyl-containing (0.1 wt%) continuous phase and thus in an encapsulated double emulsion morphology onto an amino-silane ((3-aminopropyl)trimethoxysilane)-pre-functionalized glass surface. These droplets were stable and could freely move on the substrate, however upon addition of small quantities (0.05 wt%) of the HC-surfactant Triton, the droplets assumed a Janus emulsion morphology. Followed by an exposure of the HC-W interface, the crown ether receptors bound to the NH_3^+ groups at the surface, which caused a tilting of the double-emulsion droplets out of their gravitational alignment and ultimately a spontaneous rupture of the droplet network. The latter could be attributed to the generation of a locally lipophilic surface upon complexation of the NH_3^+ functionalities that caused a wetting of the emulsions. The strong anchoring of the crown ether modalities to the emulsion droplets in these experiments was attributed to the preferred partitioning of these

**ADVANCED
SCIENCE NEWS**
www.advancedsciencenews.com

**ADVANCED
FUNCTIONAL
MATERIALS**
www.afm-journal.de

Figure 4. A) Schematic representations and optical micrographs of the behavior of double emulsion droplets sitting on a glass surface functionalized with (3-aminopropyl)trimethoxysilane. After addition of the HC surfactant Triton, the droplets decorated with crown ether surfactants bound to the NH_3^+ groups at the glass surface, which caused them to tilt, followed by a spontaneous destruction of the droplet network. B) Schematic representations and optical micrographs of the crown ether-functionalized Janus droplets on a mixed functionalized glass surface (3-(2,3-epoxypropoxy)-propyl]-trimethoxysilan/3-aminopropyl)trimethoxysilane 80:20), where interfacial supramolecular complexation led to a tilting of the droplets and a re-orientation of the latter upon addition of a competitive hydrophilic ammonium compound (2-[2-(3-aminopropoxy)ethoxy]ethan-1-ol).

compounds inside the HC-phase of the emulsion droplets as opposed to an extraction into the aqueous continuous phase, as revealed by ^{1}H-NMR-based phase partitioning investigations (Figures S30–S32, Supporting Information). **Figure 4**A displays the supposed mechanism along with micrographs of the wetting of the glass surface with the dye-containing droplet phase upon destruction of the droplets. In line with the dependency of the droplet morphology on the different chemical equilibrium-driven processes, such a supramolecular surface-interaction triggered payload release could also be evoked through variations in the salt concentrations in the aqueous continuous phase that similarly allowed to modulate the presentation of crown ether-functional groups at the droplet interface.

Besides a triggered rupture of the emulsions, a surface interaction-stimulated variation in the droplet alignment is of interest, e.g. in the context of controlling the unique dynamic refractive, reflective, and light-emitting optical properties via changing the orientation and tilt of the liquid-based micro-optical components. As described above, crown ether-functionalized double emulsions, before the wetting of the interface, could be tilted out of their gravitational alignment in response to supramolecular interactions with surface functionalities,

an observation that has previously been observed for direct droplet-droplet interactions.[28] To avoid droplet destabilization and to realize a reversible chemical-equilibrium-controlled tilting, crown ether-functionalized Janus emulsions were placed on substrates functionalized with mixed monolayers of the hydrophilic [3-(2,3-epoxypropoxy)-propyl]-trimethoxysilan and the active aminosilane 3-aminopropyl)trimethoxysilane (molar ratio 80:20). Here, droplets remained stable, however, tilted side-ways actuated by the complexation of surface NH_3^+ groups with the crown ether surfactants located at the upper HC-interface. The reversibility of the supramolecular interaction is outlined in Figure 4B and Figure S33, Supporting Information, which display a gravity-driven re-orientation of the droplet system upon competitive binding of the crown ethers to other hydrophilic ammonium compounds (1.5 mM of 2-[2-(3-aminopropoxy)ethoxy]ethan-1-ol) or metal ions.

3. Conclusion

In summary, we herein demonstrated the design and manipulation of anisotropically, crown ether-functionalized dynamic

biphasic emulsion droplets. Supramolecular complexation events at the liquid–liquid interface of the emulsions enabled interfacial complexation and thus triggered responses of the droplets to a variety of chemical triggers including metal ions, ammonium compounds, amino acids, antibodies, carbohydrates, as well as, amino-functionalized solid interfaces. The individual competing supramolecular recognition events, as well as, variations in the composition and effectiveness of external surfactants independently determined the dynamic droplet responses, solely controlled by the respective individual chemical equilibrium constants. Anisotropic supramolecular crown ether-functionalized bi-phase emulsion droplets thus constitute a novel type of adaptive, chemo-intelligent soft material platform that can autonomously regulate its response to multiple independent chemical binding events. We showcased how the multi-responsive nature of the droplets can be pre-programmed and orchestrated via triggered changes in the chemical environment, which may prove useful for the design of new and improved emulsion technologies including droplet-based microreactors, Janus emulsion biosensors, and triggered payload release applications.

Supporting Information

Supporting Information is available from the Wiley Online Library or from the author.

Conflict of Interest

The authors declare no conflict of interest.

Data Availability Statement

Data available in article supplementary material.

[1] a) Y. Tu, F. Peng, A. Adawy, Y. Men, L. K. E. A. Abdelmohsen, D. A. Wilson, *Chem. Rev.* **2016**, *116*, 2023; b) S. Mann, *Acc. Chem. Res.* **2012**, *45*, 2131.

[2] T. Y.-C. Tsai, Y. S. Choi, W. Ma, J. R. Pomerening, C. Tang, J. E. Ferrell, *Science* **2008**, *321*, 126.

[3] a) A. Deutsch, G. Theraulaz, T. Vicsek, *Interface Focus* **2012**, *2*, 689; b) G. Ashkenasy, T. M. Hermans, S. Otto, A. F. Taylor, *Chem. Soc. Rev.* **2017**, *46*, 2543; c) S. Mann, *Angew. Chem., Int. Ed.* **2008**, *47*, 5306.

[4] a) H. W. H. van Roekel, B. J. H. M. Rosier, L. H. H. Meijer, P. A. J. Hilbers, A. J. Markvoort, W. T. S. Huck, T. F. A. de Greef, *Chem. Soc. Rev.* **2015**, *44*, 7465; b) F. Soto, E. Karshalev, F. Zhang, B. E. F. de Avila, A. Nourhani, J. Wang, *Chem. Rev.* **2021**, unpublished, https://doi.org/10.1021/acs.chemrev.0c00999.

[5] E. Gouaux, R. MacKinnon, *Science* **2005**, *310*, 1461.

[6] a) A. L. Chang-Graham, J. L. Perry, M. A. Engevik, K. A. Engevik, F. J. Scribano, J. T. Gebert, H. A. Danhof, J. C. Nelson, J. S. Kellen, A. C. Strtak, N. P. Sastri, M. K. Estes, R. A. Britton, J. Versalovic, J. M. Hyser, *Science* **2020**, *370*, eabc3621; b) L. A. Barlow, *Development* **2015**, *142*, 3620.

[7] K. Xiao, L. Chen, R. Chen, T. Heil, S. D. C. Lemus, F. Fan, L. Wen, L. Jiang, M. Antonietti, *Nat. Commun.* **2019**, *10*, 74.

[8] W. Wickner, R. Schekman, *Science* **2005**, *310*, 1452.

[9] C. Pedersen, N. Poonia, A. Bajaj, R. Izatt, J. Bradshaw, S. Nielsen, J. Lamb, J. Christensen, S. Debabrata, *Chem. Rev.* **1967**, *89*, 7017.

[10] Z. Sun, M. Barboiu, Y.-M. Legrand, E. Petit, A. Rotaru, *Angew. Chem., Int. Ed.* **2015**, *54*, 1447314477.

[11] a) L. Wang, L. Cheng, G. Li, K. Liu, Z. Zhang, P. Li, S. Dong, W. Yu, F. Huang, X. Yan, *J. Am. Chem. Soc.* **2020**, *142*, 2051; b) X. Ji, J. Li, J. Chen, X. Chi, K. Zhu, X. Yan, M. Zhang, F. Huang, *Macromolecules* **2012**, *45*, 6457; c) G. W. Gokel, W. M. Leevy, M. E. Weber, *Chem. Rev.* **2004**, *104*, 2723.

[12] a) R. Merindol, A. Walther, *Chem. Soc. Rev.* **2017**, *46*, 5588; b) H. Löw, E. Mena-Osteritz, K. M. Mullen, C. M. Jäger, M. von Delius, *ChemPlusChem* **2020**, *85*, 1008.

[13] R. V. Balaj, L. D. Zarzar, *Chem. Phys. Rev.* **2020**, *1*, 011301.

[14] a) M. Pavlovic, M. Antonietti, L. Zeininger, *Chem. Commun.* **2021**, *57*, 1631; b) C. A. Zentner, F. Anson, S. Thayumanavan, T. M. Swager, *J. Am. Chem. Soc.* **2019**, *141*, 18048; c) M. Pavlovic, M. Antonietti, B. V. K. J. Schmidt, L. Zeininger, *J. Colloid Interface Sci.* **2020**, *575*, 88; d) D. Patra, C. Pagliuca, C. Subramani, B. Samanta, S. S. Agasti, N. Zainalabdeen, S. T. Caldwell, G. Cooke, V. M. Rotello, *Chem. Commun.* **2009**, *28*, 4248.

[15] S. Djalali, B. D. Frank, L. Zeininger, *Soft Matter* **2020**, *16*, 10419.

[16] a) K. H. Ku, B. R. McDonald, H. Vijayamohana, C. A. Zentner, S. Nagelberg, M. Kolle, T. M. Swager, *Small* **2021**, *17*, 2007507; b) A. E. Goodling, S. Nagelberg, B. Kaehr, C. H. Meredith, S. I. Cheon, A. P. Saunders, M. Kolle, L. D. Zarzar, *Nature* **2019**, *566*, 523; c) A. Concellón, C. Zentner, T. M. Swager, *J. Am. Chem. Soc.* **2019**, *141*, 18246.

[17] S. Nagelberg, L. D. Zarzar, N. Nicolas, K. Subramanian, J. A. Kalow, V. Sresht, D. Blankschtein, G. Barbastathis, M. Kreysing, T. M. Swager, M. Kolle, *Nat. Commun.* **2017**, *8*, 14673.

[18] a) B. D. Frank, M. Antonietti, L. Zeininger, *Macromolecules* **2021**, *54*, 981; b) Y. Guo, Y. Fang, K. Jia, Y. Yu, L. Yu, H. Li, J. Zhang, X. Zheng, L. Huang, W. Wen, Y. Mai, *Macromol. Rapid Commun.* **2021**, *42*, 2100085; c) B. D. Frank, M. Perovic, S. Djalali, M. Antonietti, M. Oschatz, L. Zeininger, *ACS Appl. Mater. Interfaces* **2021**, *13*, 32510.

[19] a) D. Fong, T. M. Swager, *J. Am. Chem. Soc.* **2021**, *143*, 4397; b) M. Pavlovic, H. K. R. R. Babu, S. Djalali, M. Vranes, V. Radonic, L. Zeininger, *Anal. Chem.* **2021**, *93*, 9390; c) J. Li, S. Savagatrup, Z. Nelson, K. Yoshinaga, T. M. Swager, *Proc. Natl. Acad. Sci. U. S. A.* **2020**, *117*, 11923.

[20] L. D. Zarzar, V. Sresht, E. M. Sletten, J. A. Kalow, D. Blankschtein, T. M. Swager, *Nature* **2015**, *518*, 520.

[21] a) S. Shinkai, K. Torigoe, O. Manabe, T. Kajiyama, *J. Am. Chem. Soc.* **1987**, *109*, 4458; b) T. Liu, C. Bao, H. Wang, L. Fei, R. Yang, Y. Long, L. Zhu, *New J. Chem.* **2014**, *38*, 3507.

[22] F. Arnaud-Neu, R. Delgado, S. Chaves, *Pure Appl. Chem.* **2003**, *75*, 71.

[23] P. Thordarson, *Chem. Soc. Rev.* **2011**, *40*, 1305.

[24] a) X. Yan, R. M. Bain, R. G. Cooks, *Angew. Chem., Int. Ed.* **2016**, *55*, 12960; b) A. Fallah-Araghi, K. Meguellati, J.-C. Baret, A. El Harrak, T. Mangeat, M. Karplus, S. Ladame, C. M. Marques, A. D. Griffiths, *Phys. Rev. Lett.* **2014**, *112*, 028301.

[25] A. M. Kolodziejczyk, M. Manning, *J. Org. Chem.* **1981**, *46*, 1944.

[26] a) L. Zeininger, S. Nagelberg, K. S. Harvey, S. Savagatrup, M. B. Herbert, K. Yoshinaga, J. A. Capobianco, M. Kolle, T. M. Swager, *ACS Cent. Sci.* **2019**, *5*, 789; b) Q. Zhang, L. Zeininger, K.-J. Sung, E. A. Miller, K. Yoshinaga, H. D. Sikes, T. M. Swager, *ACS Sens.* **2019**, *4*, 180.

[27] T. D. James, K. R. A. Samankumara Sandanayake, S. Shinkai, *Angew. Chem., Int. Ed.* **1996**, *35*, 1910.